RNA (1996), 2:718–732. Cambridge University Press. Printed in the USA.

Kinetic pathway for folding of the *Tetrahymena* ribozyme revealed by three UV-inducible crosslinks

WILLIAM D. DOWNS[1] and THOMAS R. CECH

Department of Molecular, Cellular and Developmental Biology, Howard Hughes Medical Institute, University of Colorado, Boulder, Colorado 80309-0215, USA

ABSTRACT

The kinetics of RNA folding were examined in the L-21 ribozyme, an RNA enzyme derived from the self-splicing *Tetrahymena* intron. Three UV-inducible crosslinks were mapped, characterized, and used as indicators for the folded state of the ribozyme. Together these data suggest that final structures are adopted first by the P4–P6 independently folding domain and only later in a region that positions the P1 helix (including the 5′ splice site), a region whose folding is linked to that of a portion of the catalytic core. At intermediate times, a non-native structure forms in the region of the triple helical scaffold, which connects the major folding domains. At 30 °C, the unfolded ribozyme passes through these stages with a half-life of 2 min from the time magnesium cations are provided. At higher temperatures, the half-life is shortened but the order of events is unchanged. Thermal melting of the fully folded ribozyme also revealed a multi-stage process in which the steps of folding are reversed: the kinetically slowest structure is the least stable and melts first. These structures of the ribozyme also bind Mg^{2+} cooperatively and their relative affinity for binding seems to be a major determinant in the order of events during folding. Na^{+} can also substitute for Mg^{2+} to give rise to the same crosslinkable structures, but only at much higher concentrations. Specific binding sites for Mg^{2+} may make this cation particularly efficient at electrostatic stabilization during folding of these ribozyme structures.

Keywords: folding domain; group I intron; metal cations; RNA folding problem; tertiary structure; thermal melting

INTRODUCTION

Group I introns comprise a family of RNAs that show conservation in structure (Davies et al., 1982; Michel & Dujon, 1983) and are all spliced from their precursor transcript by the same two-step reaction (Cech, 1988). In many cases, group I introns have been shown to be self-splicing, that is, the RNA alone possesses all of the catalytic machinery necessary for both steps of splicing. Shortened versions of group I introns can also be constructed to carry out cleavage of an RNA substrate in *trans* in a reaction that recapitulates the first step of splicing (Zaug et al., 1988; Michel et al., 1992). These reactions can occur with multiple turnover; thus, the RNA is behaving as a true RNA enzyme. These introns and RNA enzymes are collectively known as group I ribozymes.

A region known as the core is conserved in both sequence and secondary structure among group I introns (Waring & Davies, 1984; Michel & Westhof, 1990) and has proven to be crucial for activity (Burke et al., 1986; Flor et al., 1989; Couture et al., 1990; Michel et al., 1990; Pyle et al., 1992). Phylogenetic comparison of core sequences among group I introns has been used to build a three-dimensional model for the active site (Michel & Westhof, 1990). Experimental approaches to the three-dimensional structure adopted by group I ribozymes have used probes for solvent accessibility (Latham & Cech, 1989; Heuer et al., 1991; Weeks & Cech, 1995), chemical modification of bases (Jaeger et al., 1993; Murphy & Cech, 1993), chemical probes bound as substrate into the ribozyme (Wang & Cech, 1992; Wang et al., 1993), and electron microscopy (Murphy et al., 1994).

Both the phylogenetic comparisons and the physical approaches contribute to our understanding of the

Reprint requests to: Thomas R. Cech, Department of Chemistry and Biochemistry, Howard Hughes Medical Institute, University of Colorado, Boulder, Colorado 80309-0215, USA; e-mail: cech@colorado.edu.

[1] Present address: Fred Hutchinson Cancer Research Center, Division of Basic Sciences, Seattle, Washington, 98104, USA; e-mail: wdowns@fred.fhcrc.org.

fully folded RNA, competent for self-splicing or catalysis. It is only recently that studies have addressed the time-dependent pathway of ribozyme folding (Bevilacqua et al., 1992; Jaeger et al., 1993; Zarrinkar & Williamson, 1994; Banerjee & Turner, 1995; Weeks & Cech, 1996). The following experiments utilize UV crosslinks as probes for following the process of folding of the *Tetrahymena* group I ribozyme.

In UV-inducible crosslinking, the folded RNA is subjected to short-wave UV irradiation (λ_{max} = 254 nm). Aromatic electrons of the heterocyclic bases are excited by the UV irradiation and can form new chemical bonds with other nucleotides. In some instances, the three-dimensional structure of a folded RNA holds pairs of nucleotides in a favorable orientation such that formation of a specific crosslink is promoted (Delaney et al., 1974; Brimacombe, 1986; Ofengand et al., 1986; Stern et al., 1988; Behlen et al., 1992; Wasserman & Steitz, 1992).

One UV-inducible crosslink that occurs within the *Tetrahymena* ribozyme has been described previously (Downs & Cech, 1990). It occurs near the base of the P1 duplex, which contains the 5′ splice site. Furthermore, the nucleotides of this crosslink were found to play a role in positioning P1 and promoting accurate cleavage at the 5′ splice site during the first step of splicing (Downs & Cech, 1994).

Formation of such crosslinks depends upon the three-dimensional structure of the RNA, therefore they can be utilized as an assay for folded structure. The following experiments make use of three UV-inducible crosslinks to follow folding of the *Tetrahymena* ribozyme. The results lead to a model for part of the pathway by which the ribozyme assumes its final active structure.

RESULTS

Intramolecular crosslinks of the *Tetrahymena* ribozyme

When the fully renatured *Tetrahymena* ribozyme, L-21 *Sca* I, was subjected to short-wave UV irradiation (λ_{max} = 254 nm), it was converted into a number of crosslinked photoproducts that migrated more slowly during electrophoresis on a denaturing 5% polyacrylamide gel (Fig. 1). These crosslinked products were named Tet-1 through Tet-5, according to how severely each of their migrations was retarded. Formation of these crosslinks did not depend upon the concentration of RNA over a 10,000-fold range (10^{-4}–1.0 mg/mL), suggesting that the crosslinking reaction was intramolecular (data not shown). Therefore, formation of a

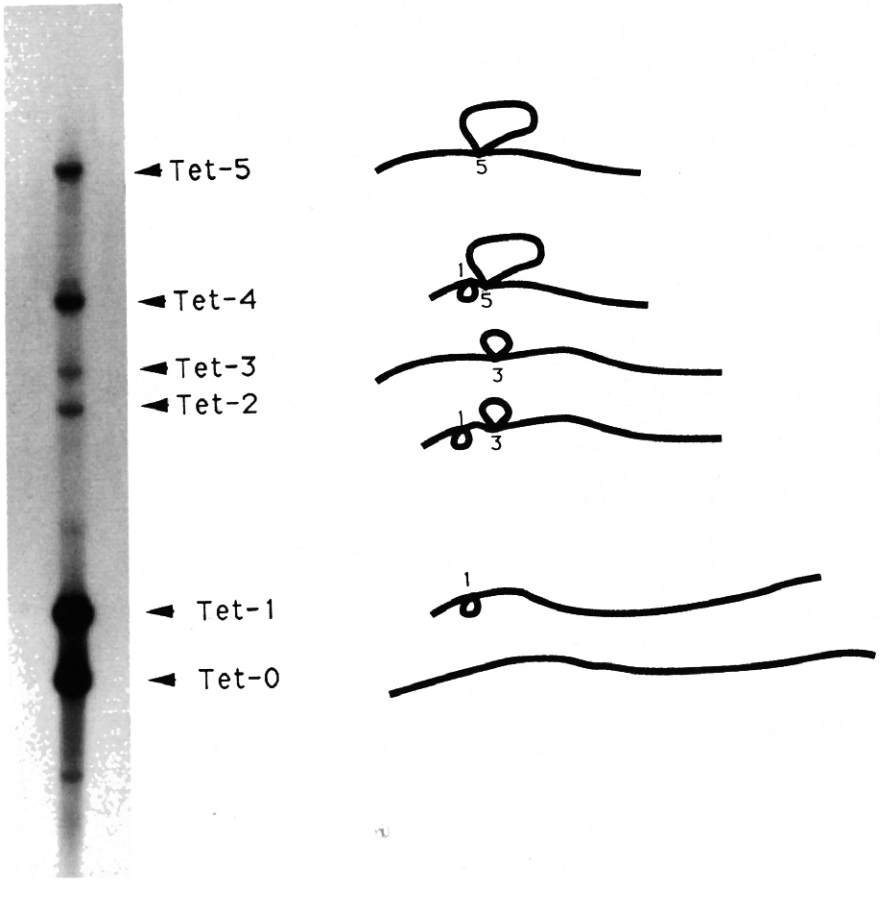

FIGURE 1. Photoproducts generated in the *Tetrahymena* ribozyme under standard crosslinking conditions. Following UV irradiation of renatured L-21 *Sca* I ribozyme, five photoproducts are generated that display retarded migration on a denaturing gel (7 M urea/5% (1:29) bis-acrylamide:acrylamide) relative to the migration of the uncrosslinked ribozyme (Tet-0). As shown on the right, each of these photoproducts contains a different combination of three crosslinks and each crosslink introduces a loop into the otherwise linear molecule. Numbers label each of the crosslinks that occur within a given photoproduct: 1, Tet-1; 3, Tet-3; 5, Tet-5.

crosslink is expected to introduce a loop structure into the otherwise linear RNA (Fig. 1).

The methods for mapping the crosslinks have been described in detail previously (Downs & Cech, 1990). Partial alkali hydrolysis and enzymatic sequencing were used to determine the 5′ partner of each crosslink. To determine the 3′ partner of each crosslink, primer extension reactions were conducted using the RNA photoproduct as a template and AMV reverse transcriptase as the polymerase. Stops in extension are expected to occur one nucleotide 3′ of the crosslinked nucleotide within the photoproduct-template.

Crosslinks were mapped in three regions of the *Tetrahymena* ribozyme. The Tet-1 crosslink has been described previously (Downs & Cech, 1990, 1994) and is depicted in Figure 2. Primer extension resulted in a pair of stops when the Tet-3 photoproduct served as template. Tet-3 therefore may represent a pair of photoproducts that do not resolve on the denaturing gels used. Thus, in one photoproduct, A122 crosslinks to

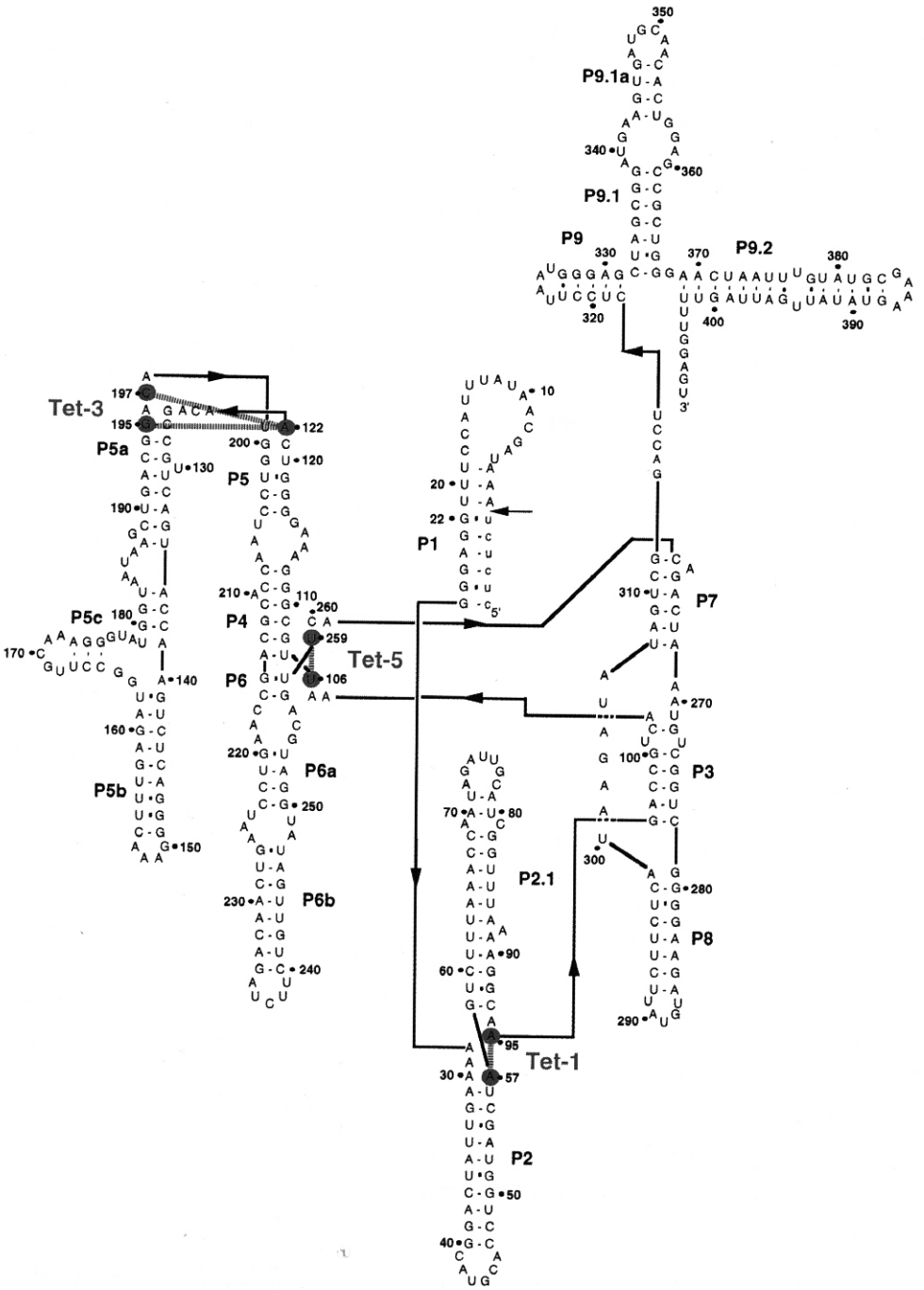

FIGURE 2. UV-inducible crosslinks mapped in photoproducts of the *Tetrahymena* ribozyme are shown on a secondary structure. The secondary structure is according to Cech et al. (1994). The BGTZ *Sca* I transcript is shown here with only the last 6 nt of its 5′ exon. An arrow near P1 indicates the site of cleavage during the first step of splicing. The L-21 *Sca* I ribozyme has its 5′ end at G22, but is otherwise identical to the BGTZ *Sca* I transcript.

A196. In the other photoproduct, A122 instead crosslinks to A198. The two Tet-3 crosslinks form across the internal loop between P5 and P5a (Fig. 2). Mutational analysis, chemical probing, and electron microscopy of this extended P5 stem all indicate that the internal loop serves as a point of bending in an otherwise helical structure (Murphy & Cech, 1993; Murphy et al., 1994). Consistent with this, the Tet-3 crosslinks suggest that nucleotides on opposite ends of the loop are brought together in the folded structure. The Tet-5 crosslink occurs within the catalytic core of the ribozyme (Fig. 2). However, the structure implied by the Tet-5 crosslink contradicts a structure already proposed for this region of the ribozyme (see the Discussion).

Two other photoproducts resulted from the UV irradiation of the *Tetrahymena* ribozyme. The Tet-2 photoproduct proved to be the consequence of the Tet-1 and Tet-3 crosslinks occurring in the same transcript. The Tet-4 photoproduct results from both the Tet-1 and Tet-5 crosslinks occurring in the same transcript.

When UV irradiation was carried out for extended periods of time, up to 80% of the starting material could be converted into photoproducts containing the Tet-1 crosslink, 28% containing Tet-3, and 23% containing Tet-5 (data not shown; Downs, 1993). We found that the extent to which the RNA could be converted to photoproducts was limited by photodegradation, therefore these numbers represent minimum estimates of the fraction of molecules in a conformation competent for forming each of the three crosslinks. In the remaining discussion, we make the assumption that this less-than-total crosslinking is due to incomplete conversion of a major conformer of the RNA rather than complete crosslinking of a minor conformer.

Relevance of each crosslink to the active structure of the ribozyme

Each crosslink depends upon a folded structure (see Thermal melting and Mg^{2+} binding, below). However, it is always possible that a crosslink occurs only in a fraction of the ribozyme molecules that have adopted an alternative, inactive conformation. The most straightforward means of testing this question is to look for activity in molecules containing each of the crosslinks. This test is based on the assumption that each crosslink will serve to lock at least a portion of the molecule into the conformation in which it occurred. Therefore, a crosslink characteristic of an inactive conformation will inactivate the molecule.

Crosslinks were introduced into BGTZ *Sca* I, a T7 transcript possessing a 5′ exon and the *Tetrahymena* intron. This 5′ exon + intron RNA will ordinarily undergo a single reaction, the first step of splicing, and be converted to the products 5′ exon and intron. During the course of this reaction, a radiolabeled guanosine was provided in solution. This nucleotide is expected to be incorporated at the 5′ end of the intron product (Cech et al., 1981). By following this self-processing reaction, it is possible to be sure the product (the intron) still contains the crosslink, and therefore any activity observed is not due to spontaneous reversal or breakdown of the crosslink.

The [α-^{32}P]GTP-labeling experiment generated products that comigrated with the linear intron photoproducts Tet-0 (UV-irradiated but uncrosslinked), Tet-1, Tet-2, and Tet-3 (Fig. 3). Therefore, the precursor remains active following UV irradiation (Tet-0) and

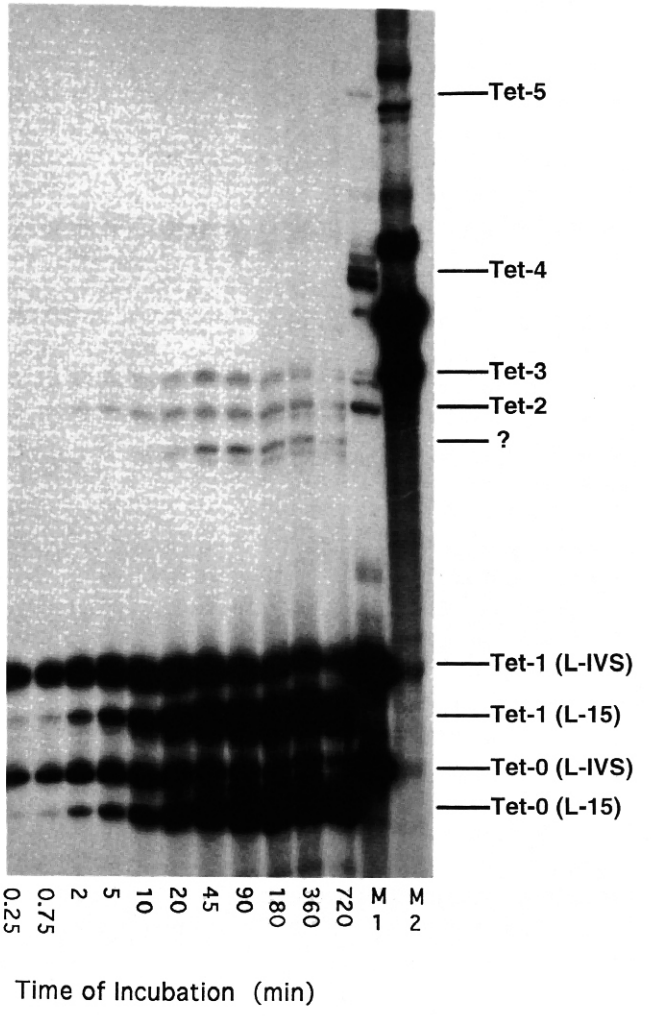

FIGURE 3. Time course of self-processing of UV-irradiated precursor RNA assessed by [α-^{32}P]GTP-labeling of the excised intron. An unlabeled precursor consisting of the 5′ exon + intron (BGTZ *Sca* I) was heat-renatured and UV-irradiated. The irradiated precursor was then combined with [α-^{32}P]GTP and incubated at 42 °C. Aliquots were taken at the times shown and loaded on a denaturing gel (7 M urea/5% (1:29) bis-acrylamide:acrylamide). Doublets presumably arise when excised intron RNA undergoes further self-processing to give an L-15 form (missing 15 nt from its 5′ end; Zaug et al., 1984). Lane M1 was loaded with [α-^{32}P]ATP body-labeled linear intron that had been UV-irradiated. These photoproducts serve as markers for [α-^{32}P]GTP-labeled products. Lane M2 was loaded with [α-^{32}P]ATP body-labeled precursor that had been UV-irradiated to show the variety of photoproducts that exist at the beginning of the self-processing reaction and that may be [α-^{32}P]GTP-labeled.

if it contains the crosslink Tet-1, Tet-3, or the combination Tet-1 and Tet-3 (i.e., Tet-2). No products were observed that comigrated with the Tet-4 or Tet-5 photoproducts. This suggests that the crosslink Tet-5 is incompatible with the active structure, or that the Tet-5 structure may be compatible, but is simply not adopted by the precursor BGTZ *Sca* I as it is by the L-21 *Sca* I enzymatic form. Another labeled product migrates just below the Tet-2 product on the denaturing gel. Its identity and the precursor photoproduct from which it is derived are unknown. Because this band has not been observed before, it suggests that the BGTZ *Sca* I precursor can adopt a crosslinkable conformation that is active, but is not abundant among renatured L-21 *Sca* I molecules.

In a separate experiment (not shown), uniformly labeled photoproducts of the BGTZ *Sca* I ribozyme were recovered from a gel. The recovered RNAs were then renatured and incubated in the presence of guanosine. This permitted us to measure the conversion of the crosslinked precursor to product (excised intron) over time. Because the label was included in the precursor, high concentrations of unlabeled guanosine (500 μM) could be used in the reaction. Three of the precursor photoproducts displayed the relative retardation in gel migration and yielded products of the appropriate size to be Tet-0, Tet-1, and Tet-2 precursors. Again, the Tet-0 precursor demonstrated that UV irradiation alone does not inactivate the self-processing activity of the RNA. The Tet-1 precursor actually underwent self-processing at a faster rate than the uncrosslinked (Tet-0) precursor and reacted to a greater extent. This suggests that the Tet-1 crosslink is not only compatible with the active structure, but aids in the folding or stabilization of the precursor upon renaturation, or disfavors misfolding in the UV-damaged RNA. The Tet-2 precursor was the least active of the precursors, but still reacted at approximately 75% the rate of the uncrosslinked, Tet-0, precursor. The Tet-2 precursor is expected to contain both the Tet-1 and Tet-3 crosslinks. Therefore, both of these crosslinks are compatible with the active structure. No precursor photoproduct was observed that yielded Tet-4 or Tet-5 linear intron as a reaction product.

Folding occurs in stages

The purpose of characterizing the Tet-1, Tet-3, and Tet-5 crosslinks was to use them as indicators of the L-21 *Sca* I ribozyme's folded state during renaturation. Both cations (namely Mg^{2+}) and elevated temperature are needed to permit the ribozyme to fold into a homogeneous, active structure (Herschlag & Cech, 1990; Walstrum & Uhlenbeck, 1990). When UV-irradiation was performed after various times of renaturation at 30 °C, the same collection of photoproducts generated upon complete renaturation and irradiation at 0 °C were formed (Fig. 4). Table 1 displays the half-lives ($t_{1/2}$) with which the ribozyme was converted into photoproducts containing Tet-1, Tet-3, and Tet-5.

A number of new photoproducts appeared and disappeared during the renaturation procedure at 30°, 40°, and 50 °C. For convenience, each of these photoproducts was named according to the previously named photoproduct that occurred just below it and then was given a letter designation (e.g., Tet-1a is a novel photoproduct migrating above Tet-1 on a denaturing gel).

Plots of the fraction of molecules yielding a given crosslink (Tet-1, Tet-3, or Tet-5) versus the time of renaturation are shown in Figure 5 at each of three temperatures. Photoproducts containing the Tet-1 and Tet-3 crosslinks appeared gradually and plateaued in abundance. This is the behavior expected if both crosslinks were the products of the final, active conformation of the ribozyme. Interestingly, the Tet-1a photoproduct showed a similar behavior (data not shown; Downs, 1993). It may represent an active structure as well. However, in previous studies, this photoproduct was neglected because the signal from this band was obscured by the larger band of the Tet-1 photoproduct that migrates so close to it.

As should be expected, the plateau for formation of each of these photoproducts occurred earlier at higher temperatures, indicating that the process of renaturation was speeded up. The photoproducts were observed to form in the same order at these elevated temperatures. The final stage observed was formation of Tet-1, which occurred with a half-life of 120 s at 30 °C (Table 1). At 40 °C and 50 °C, Tet-1 formation occurred with shortened half-lives of 51 s and 22 s, respectively. This temperature dependence corresponds to an activation energy of 17 ± 2 kcal/mol for formation of Tet-1.

Other photoproducts, such as Tet-5, showed a peak abundance, rather than a plateau, and diminished in abundance with time. This category also includes Tet-4a, Tet-3a, and Tet-1b. These are candidates for intermediates along the folding pathway.

The process of folding does not appear to be completed at 30 °C, at least within the timescale of these ex-

TABLE 1. Stability and kinetics of formation of the three crosslinkable structures within the *Tetrahymena* ribozyme.

	T_m[a] (°C)	$[Mg^{2+}]_{1/2}$[b] (mM)	$t_{1/2}$[c] (s)
Tet-1	62.0 ± 1.0	0.51 ± 0.01	120 ± 15
Tet-3	71.5 ± 1.0	0.35 ± 0.03	18 ± 6
Tet-5	71.0 ± 0.5	0.31 ± 0.03	35 ± 10

[a] Under standard crosslinking conditions (10 mM Mg^{2+}).

[b] The concentration of Mg^{2+} at which the initial rate of crosslinking is half-maximal, which is assumed to correspond to half of the molecules folded into the crosslinkable conformation (0 °C).

[c] Half-life for formation of the crosslinkable structure at 30 °C under standard crosslinking conditions (10 mM Mg^{2+}).

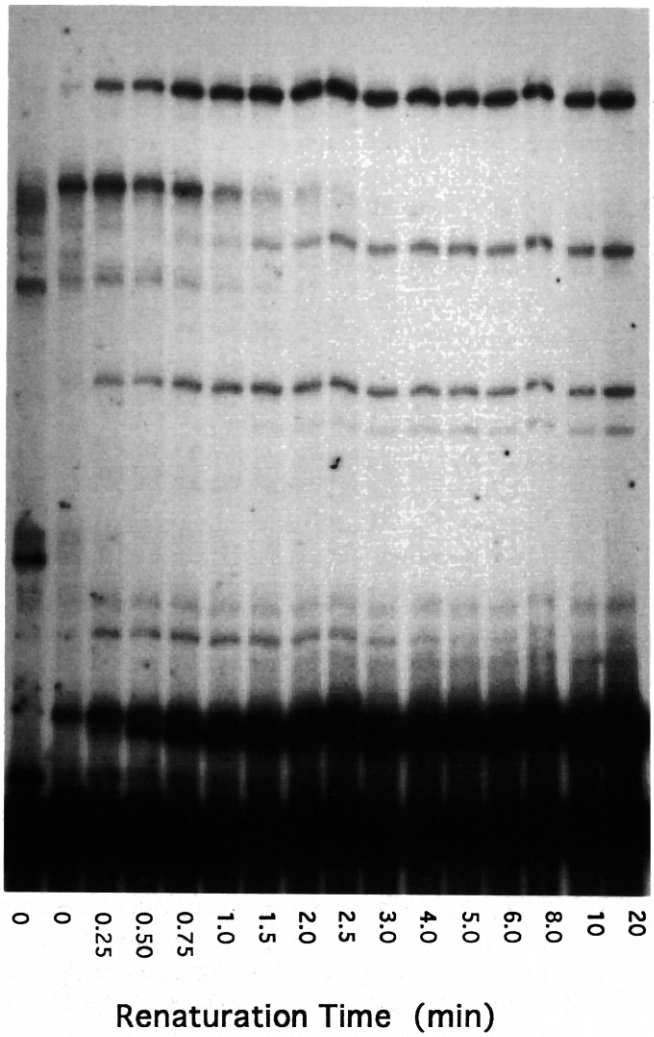

FIGURE 4. Crosslinking during ribozyme renaturation reveals different RNA substructures forming and disappearing over a time scale of minutes. Separate solutions containing [α-^{32}P]ATP body-labeled L-21 *Sca* I ribozyme and a splicing buffer concentrate were chilled (0 °C) and then combined as a total volume of 20 μL on a platform kept at a constant temperature of 30 °C. Each time point represents a different time of incubation at 30 °C prior to UV irradiation for 15 s. In each case, the time shown represents the end of the period of irradiation. The "0" lane furthest to the left is the consequence of irradiating the RNA ribozyme solution on the warmed platform, but in the absence of splicing buffer. The second "0" lane results from irradiation immediately following mixing of ribozyme and splicing buffer, but on a platform chilled to 0 °C. A portion of each irradiated sample was loaded on a denaturing gel (7 M urea/5% (1:29) bis-acrylamide:acrylamide).

periments. The Tet-5 structure persists (Fig. 5) as well as the Tet-1b structure (data not shown; Downs, 1993). Curiously, more molecules also assume the Tet-3 conformation at 30 °C than at 40 °C or 50 °C (Fig. 5). Tet-3 may therefore be just one of multiple local conformations adopted by that region in the fully renatured ribozyme and either forms faster or is favored at the lower renaturation temperature.

Thermal melting of the *Tetrahymena* ribozyme

It is also possible to follow the course of unfolding of the *Tetrahymena* ribozyme through thermal melting of the crosslinkable structures. This approach does not look at kinetic intermediates, as in the renaturation time course, but at the stability of structures in equilibrium. Aliquots of the fully renatured ribozyme were incubated for 2 min at a number of temperatures over the range 50–83 °C and UV-irradiated while still at this elevated temperature. The formation of Tet-1, Tet-3, and Tet-5 was followed at each temperature (Fig. 6). The melting temperature (T_m) of each crosslinkable structure was taken as the temperature where the rate of crosslinking is one half that seen under optimal conditions (Table 1).

The structures melt in an order opposite to their order of formation during the renaturation time course. That is, the structure that forms late during renaturation, Tet-1, is the first to melt from the fully folded molecule. In fact, the Tet-1 structure is lost before melting of the Tet-3 structure has even begun. The implication is that Tet-3 represents a domain that can fold independently of the Tet-1 structure. Likewise, Tet-1 and Tet-5 behave as separate structures rather than as components of a common structure. Furthermore, the transition ranges for formation of the Tet-5 structure and the melting out of the Tet-1 structure overlap very closely. This raises the possibility that Tet-1 and Tet-5 could be competing folded structures within the ribozyme. The Tet-5 conformation alone displays the unusual profile of being favored at an intermediate range of temperatures. Yet Tet-3 and Tet-5 parallel each other in their melting profiles. These combined results corroborate the idea that Tet-5 reflects a local conforma-

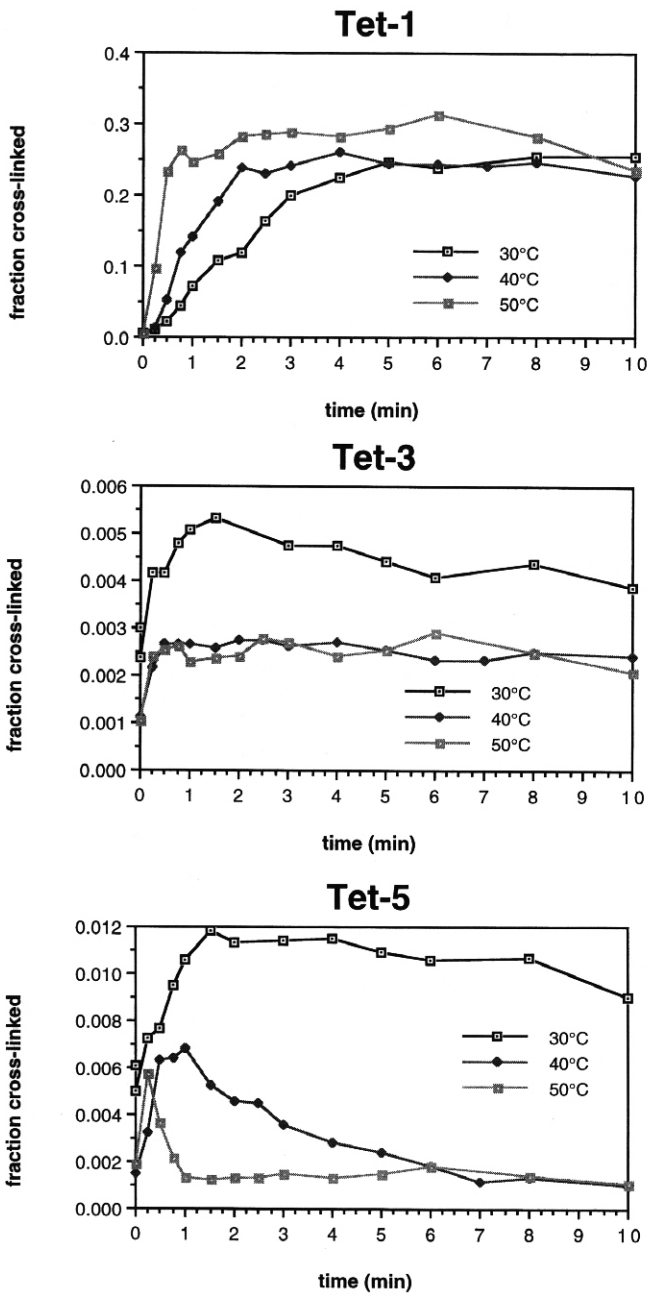

FIGURE 5. Formation of each photoproduct of the *Tetrahymena* ribozyme during a renaturation time course at 30 °C, 40 °C, and 50 °C. Each panel shows the fraction of total ribozyme converted to photoproducts containing a given crosslink upon UV irradiation at different points during renaturation (see Fig. 4).

tion within the core that forms during renaturation, but is then disrupted or altered in the final folded form. In the simplest interpretation, the Tet-5 crosslink occurs in ribozymes where the Tet-3 structure is fully formed, but the Tet-1 structure is not yet formed.

Folding as a function of Mg^{2+} binding

In order to fold into its final, active conformation, the *Tetrahymena* ribozyme requires divalent cations, namely magnesium cations (Grosshans & Cech, 1989; Celander & Cech, 1991). The Mg^{2+}-dependence of different crosslinkable structures in the *Tetrahymena* ribozyme was examined at equilibrium. The fraction of molecules folded into the crosslinkable conformation at each [$MgCl_2$] was determined as the initial rate of crosslinking relative to that measured under optimal splicing conditions. Crosslinking was performed at 0 °C to minimize evaporation and the consequential change in [Mg^{2+}].

The *Tetrahymena* ribozyme shows little change in its crosslinking pattern at concentrations of $MgCl_2$ from 1.0 to 20 mM (data not shown), with the exception of Tet-5, which is discussed below. Therefore, the range 0–1.0 mM $MgCl_2$ was examined in more detail for partial folding (Fig. 7A). The relative affinity of each crosslinkable structure for Mg^{2+} was judged according to the value $[Mg^{2+}]_{1/2}$ (Table 1).

All three crosslinks show a sigmoidal dependence of the crosslinkable conformation on [Mg^{2+}] (Fig. 7A). This is the mark of cooperative binding of magnesium cations during the folding of the RNA. That is, the binding of Mg^{2+} cations permits folding of the RNA, which in turn creates or raises the affinity of other sites for binding additional Mg^{2+} cations.

The Hill coefficient is an indicator of the level of cooperativity of binding. It equals the slope of the sigmoidal Mg^{2+} binding curve at the point of sharpest transition. For the Tet-1 conformation, the Hill coefficient is 7.4 ± 0.2, indicating that at least 7–8 magnesium cations are bound in folding this region near P1 into a structure that is competent for crosslinking. For the Tet-3 conformation, the Hill coefficient is 3.6 ± 0.4, indicating that at least 3–4 magnesium cations are bound in folding this region of the extended P5 domain. There are too few points in the plot of Figure 7A to determine a Hill coefficient for Tet-5.

Unlike the situation for the Tet-1 or Tet-3 conformations, the fraction of molecules that adopt the Tet-5 conformation is optimized over a narrow range of $MgCl_2$ concentrations. Higher concentrations of Mg^{2+} actually disfavor this structure, up to 20 mM. At the higher concentrations of Mg^{2+} cation (>0.6 mM), other structures must form and these out compete the Tet-5 conformation. Once again, this indicates that the Tet-5 conformation is not part of the final, active conformation.

Na^+ can in part substitute for Mg^{2+} in folding some structures within the ribozyme

All of the photoproducts generated following renaturation in the presence of Mg^{2+} were also generated when Na^+ was the only metal ion present. Because EDTA was also included in these reactions, it is unlikely that contaminating divalent cations were responsible for folding the crosslinkable structures (see the Materials and methods). A much greater molar concen-

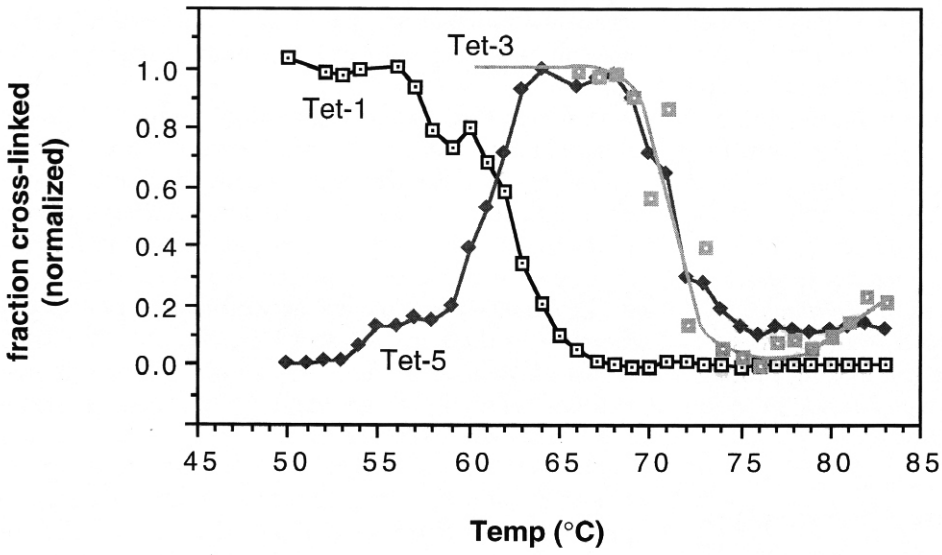

FIGURE 6. Melting profiles for three crosslinkable structures of the *Tetrahymena* ribozyme. Fully renatured ribozyme was briefly irradiated at a number of elevated temperatures. The extent of formation for each crosslink has been normalized to the greatest extent of crosslinking that was observed over the entire range. This extent of crosslinking is believed to be a measure of the initial rate of crosslinking and the fraction of ribozyme molecules in a given crosslinkable conformation.

tration of Na^+ was required to obtain the same extent of folding as could be obtained with Mg^{2+}. For instance, the extent of folding of the Tet-1 structure at 1 M Na^+ was achieved with a 4,800-fold lower molar concentration of Mg^{2+} (Fig. 7). For the Tet-3 structure, a 1,500-fold lower concentration of Mg^{2+} gave the same extent of folding. The extent of folding of Tet-3 increased linearly with Na^+ starting at the lowest concentrations, in contrast to the sigmoidal curve seen in Mg^{2+}. When Na^+ substitutes for Mg^{2+}, the metal binding sites behave as if they are uncoupled and no longer cooperate in folding the ribozyme into the Tet-3 conformation.

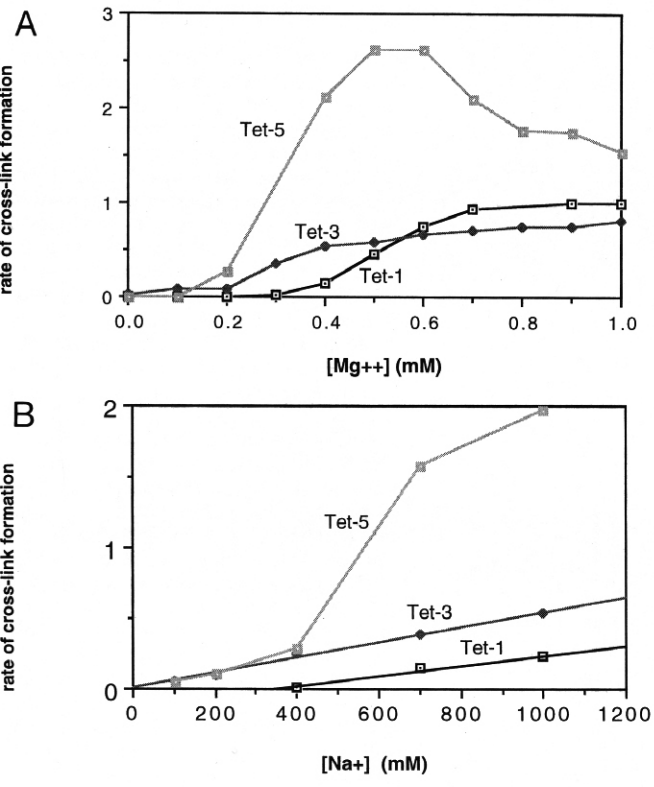

FIGURE 7. Fraction of ribozyme molecules adopting crosslinkable conformations in the presence of (**A**) varying concentrations Mg^{2+} as the only metal cation present, or (**B**) varying concentrations of Na^+ as the only metal cation present. The initial rate of crosslink formation was measured; when normalized as described below, this rate is taken to represent the fraction of molecules in a given conformational state. Each of these curves is normalized to a scale where 1.0 equals the rate of crosslink formation under metal ion conditions optimal for splicing (10 mM $MgCl_2$, 100 mM NaCl).

The fraction of molecules assuming the Tet-1 or Tet-3 conformations was less than that observed under optimal splicing conditions over the range of Na^+ concentrations tested. Meanwhile, at 1 M NaCl, the Tet-5 conformation was twice as prominent as it was under optimal splicing conditions. Once again, the Tet-5 conformation appears to be promoted by conditions that destabilize the final conformation, just as it was at low Mg^{2+} concentration and elevated temperature.

DISCUSSION

We have used UV-inducible covalent crosslinks to monitor the kinetics and thermodynamics of folding of the *Tetrahymena* ribozyme into its active tertiary structure. Crosslinking is an advantageous probe because, under single-hit conditions, it is unlikely to perturb the folding pathway, and because it can be applied under diverse temperature and ionic conditions. It has the disadvantage of revealing only a few fortuitously aligned substructures, although, in the current case, these were particularly informative regions. Furthermore, photocrosslinks occur with variable efficiency, and the fraction of crosslinked molecules provides only a lower limit of the fraction of molecules in a given conformational state.

Our data support a kinetic folding model in which folding of the P4–P6 domain precedes folding of the re-

gion that orients the P1 reaction helix, which is linked to folding of the remainder of the catalytic core. This pathway agrees with that proposed by Zarrinkar and Williamson (1994). In addition, we find misfolding of the triple helical scaffold region of the ribozyme at intermediate times during renaturation. This appears to represent an off-pathway structure; it remains possible that it is also an intermediate on a folding pathway, but if so, it is not the only folding pathway (see below, Pathway and kinetics of folding in the *Tetrahymena* ribozyme). Many other unmapped crosslinkable structures arise and disappear during the folding process, suggesting that multiple intermediates or side products accompany ribozyme renaturation.

Three crosslinks reflect structure in three regions of the ribozyme

Three UV-inducible crosslinks, Tet-1, Tet-3, and Tet-5, have been mapped in the *Tetrahymena* ribozyme L-21 *Sca* I. Each crosslink is the consequence of folding in a region of the RNA that aligns two nucleotides for a specific photochemical reaction. These crosslinks provide an assay for the folded state in three regions of the RNA.

Previous work has revealed that the nucleotides of the Tet-1 crosslink are part of a structural junction that guides the P1 helix (site of the 5′ splice site) into the catalytic core (the active site) of the *Tetrahymena* ribozyme (Downs & Cech, 1994). The region necessary for formation of Tet-1 has been modeled as containing the P3 and P7 helices of the core, as well as two helices peripheral to the core, P2 and P2.1 (Fig. 8). The Tet-1 crosslink will no longer form when the core is disrupted, even when the P2 and P2.1 helices are left intact (Downs & Cech, 1990).

The Tet-3 crosslink lies within an internal loop between P5 and P5a (Fig. 2). On one side is P5abc, a peripheral structure restricted to the C1 and C2 subgroups of group I introns (Collins, 1988; Michel & Westhof, 1990) that promotes activity of the ribozyme at low Mg^{2+} concentrations (Joyce et al., 1989; van der Horst et al., 1991). On the other side are the conserved paired regions P5, P4, and P6, which make up part of

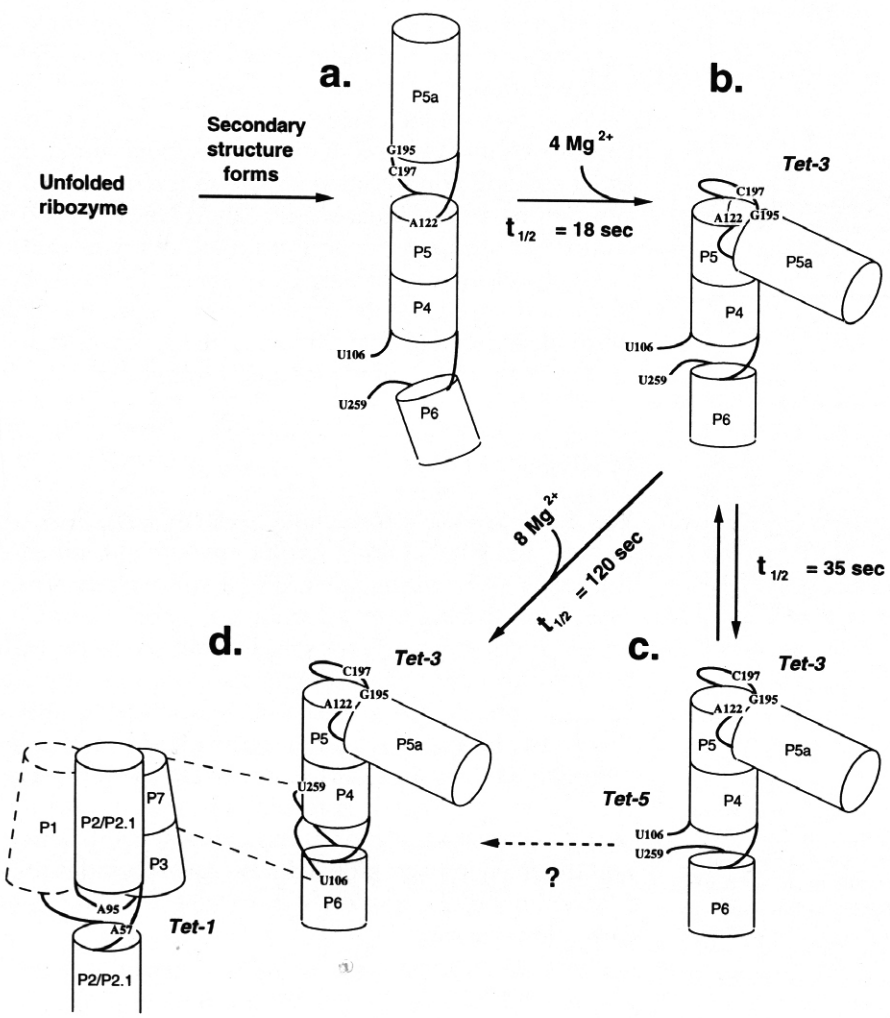

FIGURE 8. A model for the folding pathway in the *Tetrahymena* ribozyme. At each stage, a half-life ($t_{1/2}$) is given for converting the ribozyme to that folded intermediate from the point of adding $MgCl_2$ at 30 °C. *Tet-1*, *Tet-3*, and *Tet-5* indicate the presence in folding intermediates of substructures that, upon irradiation, give the crosslink indicated. **a:** Early in renaturation, the secondary structure and perhaps some tertiary structure has formed, but the crosslinking nucleotides are not in their photoreactive arrangements. **b:** Folding of the P4–P6 domain involves bending between P5 and P5a, which brings together A122, G195, and C197 into the crosslinkable conformation of Tet-3. At least four magnesium cations are bound during this step. **c:** Soon afterward, U106 and U259 come together into the non-native Tet-5 crosslinkable conformation. **d:** Final stages of folding require U106 and U259 to rearrange and participate in the triplex structure of the core, disrupting the Tet-5 arrangement. This could occur by first reverting to a prior folding intermediate, or perhaps by a direct pathway. Then core elements (including P3 and P7) participate in bringing A57 and A95 together into the Tet-1 crosslinkable structure. The P2 and P2.1 elements are labeled ambiguously, because their orientation is not known with certainty (and does not affect the conclusions herein). At least eight magnesium cations are bound during this step. The dashed outline of P1 indicates that P1 docking is a separable step; it occurs much more quickly than the folding steps studied herein (Bevilacqua et al., 1992).

the catalytic core (Couture et al., 1990; Wang et al., 1993). A bend within the P5-P5a internal loop brings P5abc in proximity with the P5-P4-P6 region (Murphy & Cech, 1993; Murphy et al., 1994), and we propose that this bend brings together the crosslinking nucleotides A122 and G195/C197 (Fig. 8). Together, all of these elements, from P5b through P6b, form an independently folding domain called P4–P6, that can be separated from the rest of the ribozyme and still adopt much of the same tertiary structure it has in the intact molecule (Murphy & Cech, 1993). By several criteria, the Tet-3 crosslink reflects the tertiary structure of the P4–P6 domain and its ability to fold independently of the remainder of the ribozyme. The ribozyme will form the Tet-3 crosslink before it is competent to form the Tet-1 crosslink during renaturation. At elevated temperatures, the Tet-1 crosslinkable arrangement is melted from the structure, yet the Tet-3 arrangement remains fully intact. The Tet-3 crosslink can also form at magnesium cation or sodium concentrations sufficiently low that formation of the Tet-1 crosslink is not observed.

Lastly, the Tet-5 crosslink comprises two nucleotides within the catalytic core, conserved among group I introns. The Tet-5 crosslink appears to represent a local structure that is not found in the final folded state of the ribozyme. One of the limitations of the crosslinking approach is that we cannot conclude that all the molecules pass through the Tet-5 conformation during folding; the fraction of molecules is ≥23% based on maximum crosslinking efficiency, consistent with it being an important state, but it remains possible that crosslinking traps and thereby accumulates a minor conformer. This crosslinkable conformation is most prevalent at a midpoint during a renaturation time course and is, for the most part, lost to other structures in the process of folding. Also, this conformation is favored under conditions that result in partial folding of the ribozyme (i.e., Tet-3 is present but Tet-1 is absent), such as elevated temperature, suboptimal concentrations of $MgCl_2$, and when Na^+ is the only metal ion present.

The Tet-5 crosslink is also incompatible with a triple helical structure in the core demonstrated to be important for activity (Michel et al., 1990; Doudna & Cech, 1995). Within the core, P4 is believed to be stacked on P6 (Kim & Cech, 1987; Michel et al., 1990; Michel & Westhof, 1990; Murphy et al., 1994), and this coaxial helix is believed to be part of the triple helix. The two nucleotides of the Tet-5 crosslink (U106 and U259) participate in this triplex as two segments of the third strand. Figure 9 shows the three-dimensional model of the triplex taken from the Michel and Westhof model for the core of the *Tetrahymena* intron (Michel & Westhof, 1990)—the two crosslinking nucleotides are proximal to one another in the triplex, but the uracil bases are separated by 8 Å and do not overlap. Therefore, they should be poor substrates for forming a crosslink (Behlen et al., 1992).

The Tet-1 and Tet-3 crosslinks represent structures consistent with the fully folded and active conformation of the *Tetrahymena* ribozyme: a fully folded conformation because the Tet-1 and Tet-3 structures, instead of appearing transiently during renaturation, plateau in their prevalence; an active conformation because a precursor containing Tet-1, or both the Tet-1 and Tet-3 crosslinks, can still undergo cleavage at the 5′ splice site. This concurs with previous results that correlate the catalytic activity of the ribozyme L-21 *Sca* I with its ability to form the Tet-1 crosslink (Downs & Cech, 1990, 1994). Meanwhile, the Tet-5 crosslink appears specific to a partially folded structure, correctly folded in the P4–P6 domain, but misfolded in the triple helix region. However, the effect of the Tet-5 crosslink on self-processing could not be assessed because this crosslink was never observed to form in the precursor. Perhaps the presence of a 5′ exon in the precursor helps to drive folding to completion.

The *Tetrahymena* ribozyme has specific Mg^{2+} binding sites

The folded regions that give rise to Tet-1, Tet-3, and Tet-5 bind Mg^{2+} at sites that show saturation at concentrations below 1.0 mM. Furthermore, the binding curves are sigmoidal, revealing that the Mg^{2+}-binding sites interact cooperatively in bringing about the folded structure. Another study looked at tertiary structure in the vicinity of P1 in the L-21 *Sca* I ribozyme by tagging the 5′ end of the ribozyme with a photocrosslinkable azido group (Wang et al., 1993). There, a Hill coefficient of 8 was assigned to the binding of Mg^{2+} cations that brings P1 into its proper position for reaction (Wang & Cech, 1994). This value is close to the Hill coefficient of 7.4 obtained here for the Tet-1 structure. (Although the present studies used ribozyme with an uncomplexed internal guide sequence rather than a full P1 duplex, it is known that P1 docks into a pre-formed site.) Both of these Hill coefficients indicate that at least eight magnesium cations are bound in a cooperative manner to establish the tertiary structure necessary for proper positioning of P1.

Crystal structures have revealed specific metal binding sites in tRNA. These sites occur where the RNA provides more than one ligand (the oxygen of a phosphate, 2′ hydroxyl group, or a bound H_2O), either at a sharp bend in the backbone or where two segments of RNA approach each other closely (Holbrook et al., 1977; Jack et al., 1977; Quigley et al., 1978; Porschke, 1986). Likewise, phosphates have been found that are likely to be involved in binding Mg^{2+} at specific sites in the folded structure of the *Tetrahymena* intron (Christian & Yarus, 1992). These candidate sites occur at the internal loop where the Tet-3 crosslink occurs, also

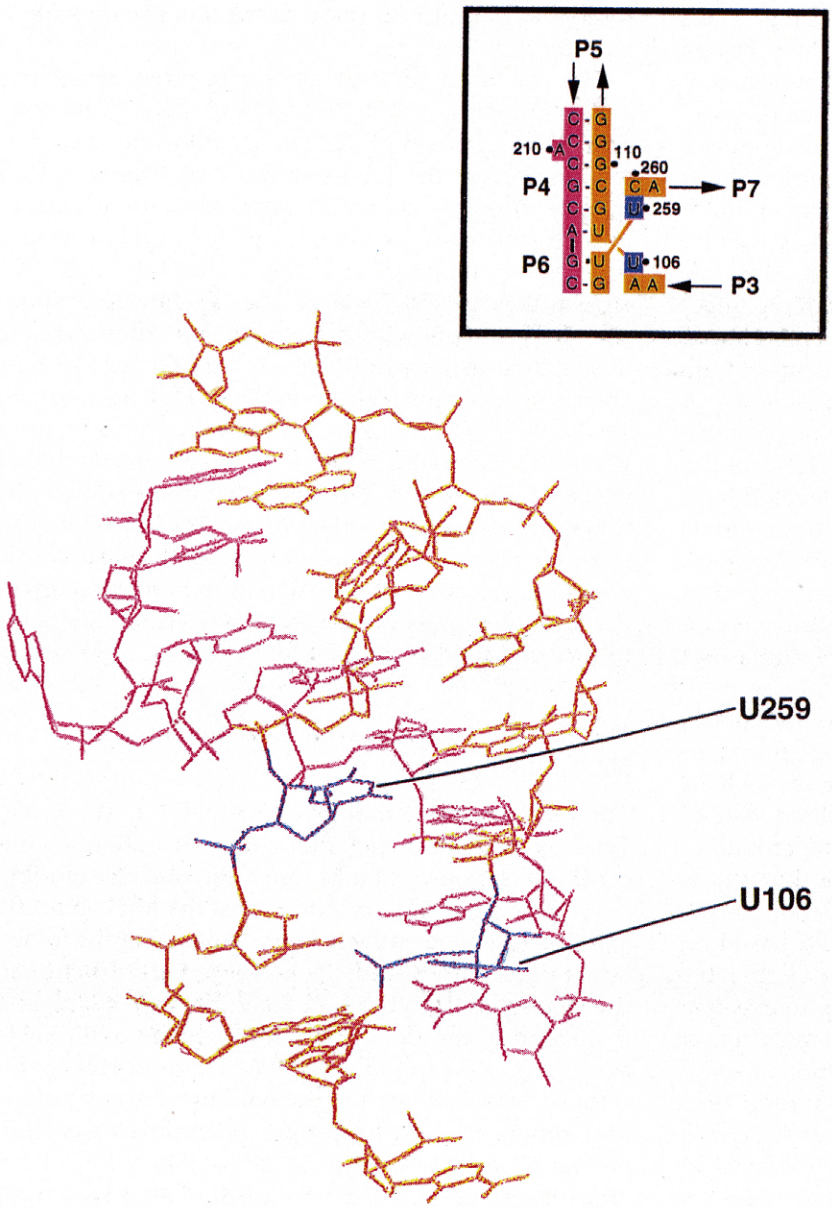

FIGURE 9. Crosslinking nucleotides of Tet-5 as they occur within the Michel and Westhof (1990) triplex model. Nucleotides of the crosslink are shown in blue and the labels (U106 and U259) point to their uracil bases. The insert near the top shows the portion of the secondary structure of the *Tetrahymena* ribozyme (from Fig. 2) that participates in the triplex. Arrows indicate the polarity of each RNA strand and point in a 5′-to-3′ direction.

within the P1, P2/2.1, and P3/7 elements that have been modeled as part of the Tet-1 structure, and within the core near both nucleotides of the Tet-5 crosslink.

Sodium cations can substitute for magnesium cations in some tertiary structures

The three crosslinkable structures obtained in the presence of $MgCl_2$ can also be achieved at extremely high concentrations of NaCl. The simplest explanation for how such different metals can serve the same role is that their purpose is one of simple electrostatics. This was initially a surprising result because previous studies with the *Tetrahymena* ribozyme indicated that only divalent cations can fold the ribozyme into the correct detailed tertiary structure, as analyzed by Fe(II)-EDTA cleavage (Celander & Cech, 1991). However, the current observations do not contradict the earlier work, because the substructures revealed by the Tet-1 and Tet-3 crosslinks may represent a subset of tertiary structures that fold in the presence of either Mg^{2+} or Na^+, whereas other tertiary structures required for the complete folded structure may rely specifically on the presence of Mg^{2+}. It is extremely reasonable that some tertiary interactions form in the absence of Mg^{2+}, because tRNA forms its tertiary structure in the absence of Mg^{2+}, but is further stabilized in its presence (Robillard et al., 1977; Boyle et al., 1980).

In addition, there are two other considerations that could apply to the Na^+ stabilized tertiary interactions: (1) The Tet-1 and Tet-3 crosslinkable structures may appear transiently in the presence of Na^+ cations alone.

The crosslinking reactions may serve to trap these unstable structures, but they remain undetected by other assays. (2) A difference between the current work and previous work is that these experiments were performed at low temperature (0 °C versus 40–50 °C), which may have served to preserve a less stable tertiary structure. Independent of the specific explanation, we conclude that the stabilization of some tertiary structures within group I ribozymes by magnesium is not unique to this cation; however, its higher charge density and site-specific binding permit it to fold this RNA cooperatively and at lower (i.e., physiological) concentrations.

Pathway and kinetics of folding in the *Tetrahymena* ribozyme

At 30 °C, the rate of renaturation was slow enough to allow us to follow the order of events carefully. Examining the renaturation time course at 40° and 50 °C demonstrated that the sequence of events at 30 °C still mirrors that observed at higher temperatures, where we are certain that renaturation goes to completion and gives active ribozyme (Herschlag & Cech, 1990).

At 40 °C, the events of folding monitored by the crosslinks are completed with a half-life of 51 s, which translates into a first-order rate constant of 0.82 min^{-1}. This is similar to the rate constants of 0.61 min^{-1} and 0.72 min^{-1} observed by Zarrinkar and Williamson (1994) for folding of this ribozyme into its fully active structure and the final conformation of the core, respectively, at 37 °C. Folding has also been examined in the *sunY* group I intron, which assumes its active conformation with a rate constant of 0.104 min^{-1} ($t_{1/2}$ = 6.67 min) at 55 °C (Jaeger et al., 1993). Formation of the Tet-1 conformation at 50 °C occurs nearly 20 times faster than this (k = 1.9 min^{-1}; $t_{1/2}$ = 22 s), yet even this value is far slower than the rapid renaturation of tRNAs, typically completed within 10 ms (Cole & Crothers, 1972; Crothers et al., 1974). The formation of tRNA secondary structure occurs at an even faster rate. Therefore, these slower rates of folding are presumably due to the higher-order structure of group I introns.

The 10 different photoproducts observed exhibit a strong correlation between their relative Mg^{2+} affinities ($[Mg^{2+}]_{1/2}$) and the order in which they form during renaturation. Putative intermediates of folding observed during renaturation also occur as photoproducts favored at low concentrations of magnesium (e.g., Tet-1a, Tet-4a, and Tet-5). (Only one photoproduct, Tet-4b, formed at low magnesium concentrations, but not during the renaturation time course.) The implication is that structures that bind Mg^{2+} with a higher affinity generally have a kinetic advantage in folding and this becomes a major factor in establishing a folding pathway.

Tet-1, Tet-3, and Tet-5, the three crosslinks that were mapped, provide a new tool for ordering the events of renaturation in the ribozyme (Fig. 8). (1) The earliest event, defined by the Tet-3 crosslink, is folding of the P4–P6 domain. Folding of P4–P6 requires bending at the internal loop between P5 and P5a (Murphy & Cech, 1993; Murphy et al., 1994). During this process of bending, we propose that the nucleotides of this internal loop adopt the Tet-3 arrangement and at least four magnesium cations are bound cooperatively. (2) During the subsequent interval in which the P4–P6 domain is assembled, but the domain that gives rise to the Tet-1 crosslink is not, the triple helical region adopts a non-native conformation in which it is competent to form the Tet-5 crosslink. Because Tet-5 rises and falls in abundance during renaturation (Fig. 5), it was initially tempting to think of the Tet-5 substructure as a folding intermediate that is subsequently replaced by the Tet-1 structure. Indeed, at 50 °C, formation of Tet-1 appears to coincide with loss of Tet-5. However, at 40 °C, formation of Tet-1 precedes loss of Tet-5 ($t_{1/2}$ = 1 min and 3 min, respectively) and, at 30 °C, the difference is even more pronounced ($t_{1/2}$ = 2 min and $\gg$ 10 min, respectively). Thus, Tet-5 appears to represent an off-pathway structure in equilibrium with a folding intermediate (Fig. 8). It remains possible that Tet-5 is on a folding pathway, but if so, it is not the only pathway (question mark in Fig. 8). (3) Formation of the Tet-1 conformation follows and requires the cooperative binding of at least eight magnesium cations. The Tet-1 crosslink is dependent on the assembly of the P3 and P7 elements of the catalytic core (Downs & Cech, 1990), so folding of the active molecule is presumably complete at this stage. Likewise, Zarrinkar and Williamson (1994) found that P3 and P7 adopt a new tertiary arrangement in the rate-limiting step of folding. (4) Once the core is formed, it remains only for the P1 helix to dock; $t_{1/2}$ = 0.3 s at 15 °C (Bevilacqua et al., 1992).

Our folding pathway is similar to that proposed by Zarrinkar and Williamson (1994), who used oligonucleotide hybridization and RNase H cleavage to monitor folding. Our states **a**, **b**, and **d** may correspond to their intermediates I_U, I_2, and I_F, respectively, based on the substructures involved, the rates of formation, and the Mg^{2+} dependence.

During renaturation, the Tet-3 structure forms at about the same time or just prior to the Tet-5 structure at three different temperatures (Fig. 5). The two structures melt simultaneously (Fig. 6), and they form at the same Mg^{2+} concentration (Fig. 7A). Thus, the non-native Tet-5 structure may depend upon the presence of the folded Tet-3 structure in order to form. As mentioned before, the Tet-3 crosslink occurs within the P4–P6 domain of the *Tetrahymena* ribozyme that has been demonstrated to fold autonomously (Celander & Cech, 1991; Murphy & Cech, 1993). Thus, it could serve as an initial structure to promote folding or misfolding in the adjacent triple helix region of the molecule.

A crosslink homologous to Tet-5 was also identified in the self-splicing group I intron of *Ankistrodesmus stipitatus* (Downs, 1993), despite extensive differences in sequence outside of the core (Davila-Aponte et al., 1991). Perhaps the Tet-5 structure is an unavoidable detour along the folding pathway.

MATERIALS AND METHODS

Preparation of ribozymes

The procedure used for transcription of RNA is described by Zaug et al. (1988) with the following exceptions. The 10× transcription buffer was composed of 200 mM Tris-HCl, pH 7.5, 75 mM $MgCl_2$, 25 mM DTT, and 10 mM spermidine. A 1-mL transcription reaction contained 100 μL 10× transcription buffer, 100 μL nucleotide mix (10 mM each GTP, ATP, UTP, CTP), 5–10 μg of linearized template (e.g., pT7L-21/*Sca* I or pBGTZ/*Sca* I; see below), and 1,000–2,000 U T7 RNA polymerase. The templates used were plasmids that had been linearized by digestion with the restriction enzyme *Sca* I. The L-21 *Sca* I ribozyme was transcribed from the linearized pT7L-21 construct (Zaug et al., 1988). The unprocessed precursor of the intron was transcribed from the pBGTZ construct. This template yields the same precursors as the pBGST7 plasmid described previously (Been & Cech, 1986). To label a transcript uniformly, only 0.25 mM ATP was included in the transcription reaction along with [α-^{32}P]ATP (600 Ci/mmol, New England Nuclear). Transcription reactions were incubated at 37 °C for 90 min (L-21 *Sca* I transcript) or at 30 °C for 60 min (BGTZ *Sca* I precursor transcript). The ribozyme was precipitated in 0.25 M NaCl plus three volumes of absolute ethanol, then gel purified. The RNA was eluted from the gel slice by rocking in 10 mM Tris-HCl, pH 7.5, 5 mM EDTA, and 0.25 M NaCl. RNA in the eluate was then precipitated with 2.5–3 volumes of absolute ethanol.

Heat-renaturation of RNA

In the snap-cool protocol, the RNA was first denatured by heating in deionized water, 1 min at 96 °C. A tenth volume of buffer was injected into the IVS solution to introduce the desired concentration of cations. Immediately thereafter, the solution was placed on ice. In the preincubation protocol, the RNA is resuspended in deionized water and a 10× buffer is added to make up 10% of the total volume. The RNA is then incubated in a 50 °C water bath for 10–20 min, then is returned to ice. Except where noted in the text, the 10× buffer was 100 mM $MgCl_2$, 1.0 M NaCl, 500 mM Tris-HCl, pH 7.5.

UV crosslinking

Except where noted in the text, crosslinking was performed in 10 mM $MgCl_2$, 100 mM NaCl, 50 mM Tris-HCl, pH 7.5. The ribozyme was crosslinked in the absence of its oligonucleotide substrate (i.e., the internal guide sequence was unoccupied), with the exception of the experiments involving the BGTZ *Sca* I ribozyme, which contains a full P1 helix. For crosslinking at low temperature (~0 °C), heat-renatured RNA samples were irradiated at a concentration of 0.2 mg/mL or less (to optimize transmittance of UV radiation) as droplets (10–50 μL) on plastic wrap over ice water. For the renaturation time courses (30°, 40°, 50 °C), the ice water was replaced with circulating water from a temperature-controlled water bath. For crosslinking at the higher temperatures for the thermal melting profiles (30–80 °C), the heat-renatured RNA solution was placed in a capped NSG quartz cuvette with a pathlength of 1 or 2 mm and submerged, except for its upper surface, in a temperature-controlled water bath. The 254-nm radiation source was a UVG-11 mineral lamp (UVP Inc.) mounted 5–10 cm above the samples. For low-temperature crosslinking, a Stratalinker 1800 (Stratagene Inc.) could also be used. The Stratalinker 1800 permits direct control of the UV dose and therefore was used when the initial rate of crosslinking needed to be determined directly. The UV-irradiated IVS was ethanol precipitated and subjected to electrophoresis on a denaturing gel (6% or greater polyacrylamide/8 M urea) for gel-purification.

Gel-purification of RNA products

The crosslinked and uncrosslinked products were excised as separate bands from a denaturing gel containing 8 M urea. The gel slices were frozen on dry ice, crushed using an ethanol-flamed, silanized glass pestle, then soaked overnight at 4 °C in 0.25 M NaCl, 10 mM Tris-HCl, pH 7.5, 1–5 mM EDTA to elute the RNA. The RNA was then precipitated with 2.5–3 volumes of absolute ethanol, washed 1–2 times with 70% ethanol, dried under vacuum, then resuspended in TE (10 mM Tris-HCl, pH 7.5, and 1 mM EDTA), or doubly distilled/deionized water.

5′ End-labeling of RNA

For 5′ end-labeling, 100 pmol of substrate RNA was incubated for 30 min at 37 °C in 50 μL of 50 mM Tris-HCl, pH 9.0, 1 mM $MgCl_2$, 0.1 mM $ZnCl_2$, 1 mM spermidine, and 5–10 U calf intestinal phosphatase (New England Nuclear). This reaction mixture was then subjected to phenol extraction, extraction with 24:1 chloroform/isoamyl alcohol (v/v). NaCl was added to a concentration of 0.25 M and the RNA was ethanol precipitated with three volumes of absolute ethanol. The RNA was resuspended in 50 μL of 50 mM Tris-HCl, pH 7.5, 10 mM $MgCl_2$, 5 mM DTT, 0.1 mM spermidine, and 0.1 mM EDTA. Twenty units of T4 polynucleotide kinase (from USB) and 7,000 Ci/mmol crude [γ-^{32}P]ATP (from ICN) were added and the mix was incubated for 30 min at 37 °C. NaCl was added to bring the concentration in the reaction to 0.25 M. The RNA was ethanol precipitated using three volumes of absolute ethanol. The pellet was dried, resuspended in loading buffer, and subjected to electrophoresis on a 7 M urea denaturing gel for gel purification. The desired band was visualized by autoradiography.

RNA sequencing and mapping of crosslinks

Enzymatic sequencing, including partial alkaline hydrolysis, was performed on 5′ end-labeled RNA according to the methods of Donis-Keller et al. (1977). Some variations were made in the procedure: 0.01 U of RNases T1 or U2 (Sankyo) or 1 U of PhyM (Bethesda Research Laboratories) were included in a 5-μL reaction mixture containing 0.2 mg/mL tRNA, and

each was incubated 15 min at 50 °C. Sequencing by primer extension was performed according to a procedure described previously (Zaug et al., 1984). Names were assigned to each crosslink to match the name of the photoproduct in which it occurs as a unique crosslink.

[α-^{32}P]GTP-labeling experiments

BGTZ *Sca* I (the *Tetrahymena* precursor) was heat-renatured by preincubation at 50 °C for 10 min in 1× splicing buffer (see Heat-renaturation of RNA). The renatured precursor was then UV-irradiated in a Stratalinker 1800 (see UV crosslinking) at 0 °C to a final energy dose of 300 mJ/cm^2. The irradiated precursor was then transferred to a 42 °C water bath for 15 s to bring it to temperature, then the self-cleavage reaction was initiated by adding [α-^{32}P]GTP in fivefold molar excess to the concentration of precursor molecules. Five-microliter aliquots were taken from the reaction at different times, combined with 5 μL of stop solution (10 M urea, 50 mM EDTA, 10 mM Tris-HCl, pH 7.5), and placed on ice. These samples were examined by electrophoresis on a 5% polyacrylamide/7 M urea denaturing gel.

Self-splicing reactions

To determine the activity of crosslinked precursors, gel-purified photoproducts of BGTZ *Sca* I (*Tetrahymena* precursor) were renatured using the 10× buffer (described under Heat-renaturation of RNA) by preincubation at 50 °C for 10 min. The renatured precursors were incubated as a 100-μL volume at 42 °C for 15 s, then reaction was initiated by addition of guanosine to a final concentration of 500 μM. Five-microliter aliquots were taken from the reaction at different times and combined with 5 μL of stop solution (10 M urea, 50 mM EDTA, 10 mM Tris-HCl, pH 7.5), and placed on ice. These samples were examined by electrophoresis on a 5% polyacrylamide/7 M urea denaturing gel.

Metal-dependence studies

L-21 *Sca* I RNA was heat-renatured by preincubation at 50 °C for 20 min in a solution containing 20 mM Tris-HCl, pH 7.5, and 0–20 mM $MgCl_2$. The concentration of $MgCl_2$ was known by precisely measuring the density of the stock solution that was then diluted to make up the different solutions used in renaturation. The renatured ribozyme was UV-irradiated for different lengths of time at low temperature (0 °C) using the Stratalinker 1800 (see UV crosslinking). For the Na^+ studies, renaturation was conducted in solutions in which $MgCl_2$ was replaced with Na^+ salts. The solutions had a sodium cation concentration of 0–1,000 mM. The Na^+ salts consisted of Na_3·EDTA and NaCl present in a 1:9 molar ratio.

Hill coefficients were determined by fitting the data points available to the equation

$$\text{Fraction crosslinked} = \frac{[Mg^{2+}]^n}{[Mg^{2+}]^n + [Mg^{2+}]^n_{1/2}},$$

using the program KaleidaGraph v. 2.1.3 (Abelbeck Software). In this equation, n is the Hill coefficient. This software package provided both the Hill coefficients and the errors quoted in the text based on the curve fits.

Quantitation

Counts contained in gels were measured using the PhosphorImager system (Molecular Dynamics, Inc.) on polyacrylamide gels that had been mounted and dried on Whatman 3M paper.

ACKNOWLEDGMENTS

We thank Jin-Feng Wang for many useful discussions concerning the analysis of crosslinks; Dan Celander and Felicia Murphy for advice and reagents for the magnesium studies; and Felicia Murphy and Joe Picirilli for guidance in computer modeling. We are also grateful to Francois Michel and Eric Westhof for sharing the coordinates for the model of the *Tetrahymena* ribozyme core prior to its publication. Art Pardi's and Barry Stoddard's research groups made both their facilities and their expertise available to us. Olke Uhlenbeck and his coworkers provided equipment and advice on this project. This work was supported by NIH grant GM-28039. T.R.C. is an Investigator, Howard Hughes Medical Institute, and an American Cancer Society Professor. We thank the W.M. Keck Foundation for their generous support of RNA research at the University of Colorado at Boulder.

Received April 3, 1996; returned for revision May 6, 1996; revised manuscript received May 14, 1996

REFERENCES

Banerjee AR, Turner DH. 1995. The time dependence of chemical modification reveals slow steps in the folding of a group I ribozyme. *Biochemistry 34*:6504–6512.

Been MD, Cech TR. 1986. One binding site determines sequence specificity of *Tetrahymena* pre-rRNA self-splicing, *trans*-splicing, and RNA enzyme activity. *Cell 47*:207–216.

Behlen LS, Sampson JR, Uhlenbeck OC. 1992. An ultraviolet light-induced crosslink in yeast tRNA^{Phe}. *Nucleic Acids Res 20*:4055–4059.

Bevilacqua PC, Kierzek R, Johnson KA, Turner DH. 1992. Dynamics of ribozyme binding of substrate revealed by fluorescence-detected stopped-flow methods. *Science 258*:1355–1358.

Boyle J, Robillard GT, Kim SH. 1980. Sequential folding of transfer RNA. A nuclear magnetic study of successively longer tRNA fragments with a common 5′ end. *J Mol Biol 139*:601–625.

Brimacombe R. 1986. The three-dimensional organization of *Escherichia coli* ribosomal RNA. In: van Knippenberg PH, Hilbers CW, eds. *Structure and dynamics of RNA*. New York: Plenum Press. pp 239–251.

Burke JM, Irvine KD, Kaneko KJ, Kerker BJ, Oettgen AB, Tierney WM, Williamson CL, Zaug AJ, Cech TR. 1986. Role of conserved sequence elements 9L and 2 in self-splicing of the *Tetrahymena* ribosomal RNA precursor. *Cell 45*:167–176.

Cech TR. 1988. Conserved sequences and structures of group I introns: Building an active site for RNA catalysis – A review. *Gene 73*:259–271.

Cech TR, Damberger SH, Gutell RR. 1994. Representation of the secondary and tertiary structure of group I introns. *Nature Struct Biol 1*:273–280.

Cech TR, Zaug AJ, Grabowski PJ. 1981. In vitro splicing of the ribosomal RNA precursor of *Tetrahymena*: Involvement of a guanosine nucleotide in the excision of the intervening sequence. *Cell 27*:487–496.

Celander DW, Cech TR. 1991. Visualizing the higher order folding of a catalytic RNA molecule. *Science 251*:401–407.

Christian EL, Yarus M. 1992. Analysis of the role of phosphate oxygens in the group I intron from *Tetrahymena*. *J Mol Biol 228*:743–758.

Cole PE, Crothers DM. 1972. Conformation changes of transfer ribonucleic acid. Relaxation kinetics of the early melting transition of methionine transfer ribonucleic acid (*Escherichia coli*). *Biochemistry 11*:4368–4374.

Collins RA. 1988. Evidence of natural selection to maintain a functional domain outside of the "core" in a large subclass of group I introns. *Nucleic Acids Res 16*:2705–2715.

Couture S, Ellington AD, Gerber AS, Cherry JM, Doudna JA, Green R, Hanna M, Pace U, Rajagopal J, Szostak JW. 1990. Mutational analysis of conserved nucleotides in a self-splicing group I intron. *J Mol Biol 215*:345–358.

Crothers DM, Cole PE, Hilbers CW, Shulman RG. 1974. The molecular mechanism of thermal unfolding of *Escherichia coli* formylmethionine transfer RNA. *J Mol Biol 87*:63–88.

Davies RW, Waring RB, Ray JA, Brown TA, Scazzocchio C. 1982. Making ends meet: A model for RNA splicing in fungal mitochondria. *Nature 300*:719–724.

Davila-Aponte JA, Huss VAR, Sogin ML, Cech TR. 1991. A self-splicing group I intron in the nuclear pre-rRNA of the green alga, *Ankistrodesmus stipitatus*. *Nucleic Acids Res 19*:4429–4436.

Delaney P, Bierbaum J, Ofengand J. 1974. Conformational changes in the thiouridine region of *Escherichia coli* transfer RNA as assessed by photochemically induced crosslinking. *Arch Biochem Biophys 161*:260–267.

Donis-Keller H, Maxam AM, Gilbert W. 1977. Mapping adenosines, guanosines, and pyrimidines in RNA. *Nucleic Acids Res 4*:2527–2538.

Doudna JA, Cech TR. 1995. Self-assembly of a group I intron active site from its component tertiary structural domains. *RNA 1*:36–45.

Downs WD. 1993. The folded structure of group I RNA enzymes as revealed by ultraviolet-inducible cross-links [thesis]. Boulder, Colorado: University of Colorado.

Downs WD, Cech TR. 1990. An ultraviolet-inducible adenosine-adenosine cross-link reflects the catalytic structure of the *Tetrahymena* ribozyme. *Biochemistry 29*:5605–5613.

Downs WD, Cech TR. 1994. A tertiary interaction in the *Tetrahymena* intron contributes to selection of the 5′ splice site. *Genes & Dev 8*:1198–1211.

Flor PJ, Flanegan JB, Cech TR. 1989. A conserved base pair within helix P4 of the *Tetrahymena* ribozyme helps to form the tertiary structure required for self-splicing. *EMBO J 8*:3391–3399.

Grosshans CA, Cech TR. 1989. Metal ion requirements for sequence-specific endoribonuclease activity of the *Tetrahymena* ribozyme. *Biochemistry 28*:6888–6894.

Herschlag D, Cech TR. 1990. Catalysis of RNA cleavage by the *Tetrahymena thermophila* ribozyme. 1. Kinetic description of the reaction of an RNA substrate complementary to the active site. *Biochemistry 29*:10159–10171.

Heuer TS, Chandry PS, Belfort M, Celander DW, Cech TR. 1991. Folding of group I introns from bacteriophage *T4* involves internalization of the catalytic core. *Proc Natl Acad Sci USA 88*:11105–11109.

Holbrook SR, Sussman JL, Warrant RW, Church GM, Kim SH. 1977. RNA-ligand interactions: Magnesium binding sites in yeast tRNA-Phe. *Nucleic Acids Res 4*:2811–2820.

Jack A, Ladner JE, Rhodes D, Brown RS, Klug A. 1977. A crystallographic study of metal-binding to yeast phenylalanine transfer RNA. *J Mol Biol 111*:315–328.

Jaeger L, Westhof E, Michel F. 1993. Monitoring of the cooperative unfolding of the *sunY* group I intron of bacteriophage *T4*. *J Mol Biol 234*:331–346.

Joyce GF, van der Horst G, Inoue T. 1989. Catalytic activity is retained in the *Tetrahymena* group I intron despite removal of the large extension of element P5. *Nucleic Acids Res 11*:7879–7889.

Kim SH, Cech TR. 1987. Three-dimensional model of the active site of the self-splicing rRNA precursor of *Tetrahymena*. *Proc Natl Acad Sci USA 84*:8788–8792.

Latham JA, Cech TR. 1989. Defining the inside and outside of a catalytic RNA molecule. *Science 245*:276–282.

Michel F, Dujon B. 1983. Conservation of RNA secondary structure in two intron families including mitochondrial-, chloroplast- and nuclear-encoded members. *EMBO J 2*:33–38.

Michel F, Ellington AD, Couture S, Szostak JW. 1990. Phylogenetic and genetic evidence for base-triples in the catalytic domain of group I introns. *Nature 347*:578–580.

Michel F, Jaeger L, Westhof E, Kuras R, Tihy F, Xu MQ, Shub DA. 1992. Activation of the catalytic core of a group I intron by a remote 3′ splice junction. *Genes & Dev 6*:1373–1385.

Michel F, Westhof E. 1990. Modelling of the three-dimensional architecture of group I catalytic introns based on comparative sequence analysis. *J Mol Biol 216*:585–610.

Murphy FL, Cech TR. 1993. An independently folding domain of RNA tertiary structure within the *Tetrahymena* ribozyme. *Biochemistry 32*:5291–5300.

Murphy FL, Wang YH, Griffith JD, Cech TR. 1994. Coaxially stacked RNA helices in the catalytic center of the *Tetrahymena* ribozyme. *Science 265*:1709–1712.

Ofengand J, Ciesiolka J, Nurse K. 1986. Ribosomal RNA at the decoding site of the tRNA–ribosome complex. In: van Knippenberg PH, Hilbers CW, eds. *Structure and dynamics of RNA*. New York: Plenum Press. pp 273–287.

Porschke D. 1986. Mg^{++}—Inner sphere complexes at "ends" and "bends" of polynucleotides and their potential role as long range inducers of conformational changes. In: van Knippenberg PH, Hilbers CW, eds. *Structures and dynamics of RNA*. New York: Plenum Press. pp 77–85.

Pyle AM, Murphy FL, Cech TR. 1992. RNA substrate binding site in the catalytic core of the *Tetrahymena* ribozyme. *Nature 358*: 123–128.

Quigley GJ, Teeter MM, Rich A. 1978. Structural analysis of spermine and magnesium ion binding to yeast phenylalanine transfer RNA. *Proc Natl Acad Sci USA 75*:64–68.

Robillard GT, Tarr CE, Vosman F, Reid BR. 1977. A nuclear magnetic resonance study of secondary and tertiary structure in yeast $tRNA^{Phe}$. *Biochemistry 16*:5261–5273.

Stern S, Weiser B, Noller HF. 1988. Model for the three-dimensional folding of 16S ribosomal RNA. *J Mol Biol 204*:447–481.

van der Horst G, Christian A, Inoue T. 1991. Reconstitution of a group I intron self-splicing reaction with an activator RNA. *Proc Natl Acad Sci USA 88*:184–188.

Walstrum SA, Uhlenbeck OC. 1990. The self-splicing RNA of *Tetrahymena* is trapped in a less active conformation by gel purification. *Biochemistry 29*:10573–10576.

Wang JF, Cech TR. 1992. Tertiary structure around the guanosine-binding site of the *Tetrahymena* ribozyme. *Science 256*:526–529.

Wang JF, Cech TR. 1994. Metal ion dependence of active-site structure of the *Tetrahymena* ribozyme revealed by site-specific photocross-linking. *J Am Chem Soc 116*:4178–4182.

Wang JF, Downs WD, Cech TR. 1993. Movement of the guide sequence during RNA catalysis. *Science 260*:504–508.

Waring RB, Davies RW. 1984. Assessment of a model for intron RNA secondary structure relevent to RNA self-splicing—A review. *Gene 28*:277–291.

Wasserman DA, Steitz JA. 1992. Interactions of small nuclear RNA's with precursor messenger RNA during in vitro splicing. *Science 257*:1918–1925.

Weeks KM, Cech TR. 1995. Protein facilitation of group I intron splicing by assembly of the catalytic core and the 5′ splice site domain. *Cell 82*:221–230.

Weeks KM, Cech TR. 1996. Assembly of a ribonucleoprotein catalyst by tertiary structure capture. *Science 271*:345–348.

Zarrinkar PP, Williamson JR. 1994. Kinetic intermediates in RNA folding. *Science 265*:918–924.

Zaug AJ, Grosshans CA, Cech TR. 1988. Sequence-specific endoribonuclease activity of the *Tetrahymena* ribozyme: Enhanced cleavage of certain oligonucleotide substrates that form mismatched ribozyme–substrate complexes. *Biochemistry 27*:8924–8931.

Zaug AJ, Kent JR, Cech TR. 1984. A labile phosphodiester bond at the ligation junction in a circular intervening sequence RNA. *Science 224*:574–578.